Large numbers of cold positronium atoms created in laser-selected Rydberg states using resonant charge exchange

R McConnell[1], G Gabrielse[1,5], W S Kolthammer[1], P Richerme[1], A Müllers[2], J Walz[2], D Grzonka[3], M Zielinski[3], D Fitzakerley[4], M C George[4], E A Hessels[4], C H Storry[4] and M Weel[4] (ATRAP Collaboration)

[1] Department of Physics, Harvard University, Cambridge, Massachusetts 02138, USA
[2] Institut für Physik, Johannes Gutenberg-Universität and Helmholtz Institut Mainz, D-55099, Mainz, Germany
[3] IKP, Forschungzentrum Jülich GmbH, D-52425 Jülich, Germany
[4] Department of Physics and Astronomy, York University, Toronto, Ontario M3J 1P3, Canada

E-mail: hessels@yorku.ca

CrossMark

Abstract

Lasers are used to control the production of highly excited positronium atoms (Ps*). The laser light excites Cs atoms to Rydberg states that have a large cross section for resonant charge-exchange collisions with cold trapped positrons. For each trial with 30 million trapped positrons, more than 700 000 of the created Ps* have trajectories near the axis of the apparatus, and are detected using Stark ionization. This number of Ps* is 500 times higher than realized in an earlier proof-of-principle demonstration (2004 *Phys. Lett.* B **597** 257). A second charge exchange of these near-axis Ps* with trapped antiprotons could be used to produce cold antihydrogen, and this antihydrogen production is expected to be increased by a similar factor.

(Some figures may appear in colour only in the online journal)

1. Introduction

The three-body interaction of cold antiprotons ($\overline{p}$) and cold positrons (e^+) in a nested Penning trap suggested long ago [1] was used to create the first observed slow antihydrogen ($\overline{H}$) atoms [2–5], and to produce essentially all of the slow $\overline{H}$ atoms that have been studied since, including recently trapped $\overline{H}$ atoms [6–8]. The only demonstrated alternative [9] utilizes a laser-controlled charge-exchange method [10]. However, this proof-of-principle experiment generated too few atoms for further $\overline{H}$ studies (i.e., for studies of CPT symmetry and of antimatter gravity). If the production rate could be increased, this method for creating $\overline{H}$ could have advantages, and others are also now pursuing charge exchange for the production of $\overline{H}$ [11]. Charge exchange should produce more $\overline{H}$ atoms cold

enough to be trapped, since an $\overline{H}$ formed by this method is expected to have a kinetic energy close to that of the cold $\overline{p}$ from which it forms, and thus could take advantage of the recent advances in cooling $\overline{p}$ using adiabatic [12] or evaporative [13] techniques. The charge-exchange method allows for control of the binding energy of the state in which the $\overline{H}$ is formed.

In the laser-controlled charge-exchange method described in this work, excited positronium atoms (Ps*) are created when laser-excited Cs* atoms collide with trapped positrons:

$$Cs^* + e^+ \rightarrow Ps^* + Cs^+. \qquad (1)$$

In this resonant charge-exchange collision, the binding energy of the Ps* is roughly equal to that of the Cs*. The cross section for the formation of Ps* is large because the radius of the Cs* atom is large, scaling as $n^2 a_B$, where n is the principal quantum number for the Cs* and a_B is the Bohr radius. The

[5] ATRAP Collaboration Spokesperson.

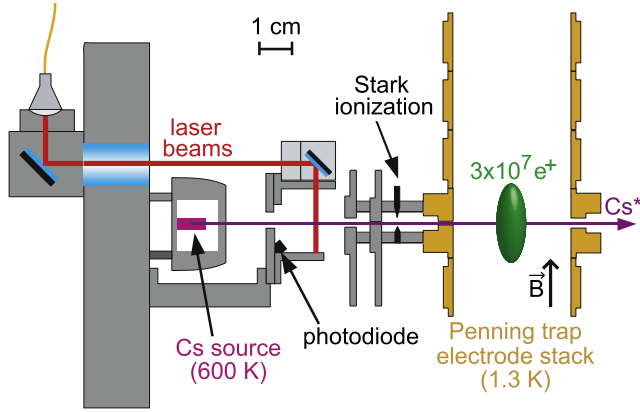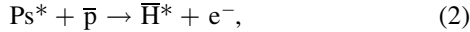J. Phys. B: At. Mol. Opt. Phys. **49** (2016) 064002

R McConnell *et al*

Figure 1. Apparatus for producing a Rydberg Cs* beam and its location relative to the Penning-trap electrodes used to confine e+ for Ps* production experiments.

Figure 2. (a) Energy levels of Cs in no field and in a 1-T field (not to scale). (b) The 1-T states near $31\,340\,\text{cm}^{-1}$ expanded. (c) The predicted relative efficiency for producing Ps* versus n state.

cross section for Ps* formation thus scales as $\sigma(\text{Ps}^*) \propto \pi a_B^2 n^4$. A proportionality constant of 9.7 is predicted by a classical-trajectory Monte Carlo calculation for zero magnetic field [10], and values of 4–6.5 are predicted for magnetic fields of 1–4 T [14].

This paper reports producing and detecting more than 700 000 Ps* that are directed near the axis of the experiment per hour-long trial of the experiment. This number is 500 times larger than in an earlier proof-of-principle demonstration [15], which required a much longer time per trial. The increase in Ps* production will be beneficial for $\overline{\text{H}}$ production, since the $\overline{\text{p}}$ for a second charge exchange

$$\text{Ps}^* + \overline{\text{p}} \rightarrow \overline{\text{H}}^* + \text{e}^-, \qquad (2)$$

would also be situated near the axis of the experiment, and, therefore, $\overline{\text{H}}$ production is expected to increase by a similar factor.

While the use of Ps* for $\overline{\text{H}}$ production is the main motivation for this work, the result presented here may also be important for other positronium studies, which might use this technique for producing Ps* atoms. Such studies could take advantage of the large numbers of Ps* atoms, the long lifetime of the Rydberg states created, and the laser control of the Ps* state produced.

2. Apparatus

The ATRAP Penning-Ioffe trap apparatus, which has been successfully used to trap large plasmas of $\overline{\text{p}}$ and e+ and to make and trap $\overline{\text{H}}$ atoms, is described extensively elsewhere [16, 17]. An electrostatic quadrupole potential (produced by applying potentials to a stack of hollow cylindrical electrodes, some of which are shown in figure 1) provides axial confinement for trapped charged particles, while radial confinement is provided by a uniform axial magnetic field, $\vec{B} = 1\,\text{T}\,\hat{z}$.

Figure 1 shows the apparatus used to produce a Cs* beam which enters the cryogenic Penning trap and initiates Ps* formation. Although any atom could in principle be used, Cs is chosen for its convenient wavelengths for laser excitation to
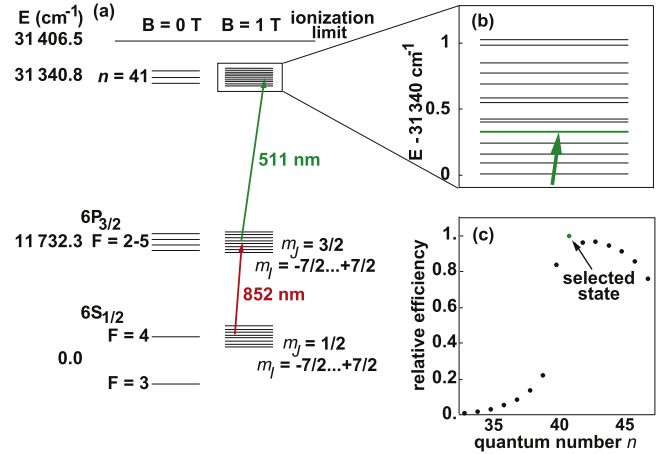
a Rydberg state. A resistively-heated source (Alvatec AS-3-Cs-150-V) sublimates a flux of Cs atoms once it reaches an operating temperature of 600 K. The source is enclosed in an aluminum box, and is further thermally isolated from the Penning-trap electrodes by radiation shielding baffles. This isolation prevents the 1.3 K trap electrodes [18] from heating by more than 1 K during an hour of continuous source operation. The Cs enters the Penning-trap region through a 0.8 mm diameter hole in one electrode. Collimation elements ensure that all ballistic Cs trajectories entering the Penning-trap region will exit through another 2.5 mm diameter hole in the far side of this electrode to prevent a buildup of Cs metal on the surfaces of electrodes. The Cs source contains enough Cs to allow for experiments throughout an 8 month beam run, without the need to warm up the cryogenic Penning-Ioffe-trap apparatus and replace the source.

Laser light to excite the Cs to a Rydberg state is coupled into the apparatus by optical fiber, and the light emerging from the fiber is collimated before passing through a quartz window to enter the 4 K ultra-high-vacuum region where it is directed downward by a mirror to intersect the Cs beam (figure 1). The diameters of the laser beams at the point of Cs excitation are approximately 1.5 mm.

Because of space constraints, this Cs* production apparatus is made small enough to slide into a 1.9 cm wide, 5.1 cm high port in one side of the Ioffe trap, while still allowing for access through this same port for 121.6 nm Lyman-α light, which will allow for possible laser cooling of trapped $\overline{\text{H}}$, and for other laser light for possible spectroscopic measurements.

3. Laser-controlled production of a Rydberg Cs beam

Cesium is excited to a Rydberg state by two lasers. A schematic of this excitation is shown in figure 2(a). An 852 nm laser excites Cs from its $6S_{1/2}$ ground state to the short-lived $6P_{3/2}$ state, while 511 nm laser light makes the second excitation to a state near $n = 41$.

In the 1-T field of the Penning trap used for this work, a diagonalization of the Hamiltonian is needed to determine the

energy levels near $31\,340\,\text{cm}^{-1}$ (near $n = 41$) shown in figure 2(b). In order to converge on the correct energies, the diagonalization includes all states with $10 < n < 60$, and includes quantum defects [19] and the magnetic Hamiltonian [20]:

$$H_B = \mu_B B_0 (g_L m_L + g_S m_S) + \frac{1}{8} \frac{e^2 B_0^2}{m_e c^2} r^2 \sin^2(\theta). \quad (3)$$

Each state in figure 2(b) is a mixture of L states, and the state with the largest D-state character in figure 2(b) (the state that has the largest electric-dipole matrix element connecting it to the $6P_{3/2}$ state) is shown in green. The 511 nm laser is tuned to excite this state.

For each value of n, there is a set of states similar to those shown in figure 2(b) and our choice of n state is influenced by several factors. The first is the size of the electric-dipole matrix element, which decreases with increasing n both because the $6P_{3/2}$–nD matrix element decreases with increasing n, and because the admixture of D-state character in any particular state (obtained by diagonalizing the Hamiltonian for the 1-T field) becomes smaller with increasing n. Because the 511 nm light is below the saturation intensity for the transition, larger electric-dipole matrix elements will enhance the excitation efficiency. The second factor is the lifetime of the Rydberg state. This lifetime increases with increasing n both because the nD lifetime increases and because of the increasing admixture of longer-lived higher-L states. The longer lifetime allows a larger fraction of the Cs^* to survive (at their 600 K thermal speeds) for the 6 cm distance of their travel from the excitation point to the e^+ plasma of figure 1. The third factor is the n^4 scaling of the cross section for charge exchange. A combination of all three factors leads to the Ps^* production efficiency versus n shown in figure 2(c). Only a small range of n values are efficient for producing Ps^*, and the state used in this work ($n = 41$) is highlighted in the figure. This choice of n is larger than that used in the proof-of-principle work [15], where the smaller distance that the Cs^* atoms needed to travel made the Cs^* lifetime a less important factor in the choice of n.

The laser system used to excite the Cs atoms is described in [21]. For the $6S_{1/2} \rightarrow 6P_{3/2}$ transition, an external-cavity diode laser provides up to 160 mW of laser power at 852 nm. As the saturation intensity for the $6S_{1/2} \rightarrow 6P_{3/2}$ transition is only $2.7\,\text{mW cm}^{-2}$, typically only 3 mW of 852 nm power is used. The laser is locked to a temperature-stabilized wavemeter, and doppler-free spectroscopy in a room-temperature Cs vapor cell allows for calibration of the wavemeter. Up to 200 mW of 511 nm light for the $6P_{3/2} \rightarrow n = 41$ transition is provided by an external-cavity diode laser at 1022 nm, which is amplified to 1 W in a tapered amplifier and frequency doubled within a cavity using a BiBO crystal. This laser is also locked to a temperature-stabilized wavemeter. The linewidth of both lasers is significantly less than the doppler width of the 600 K Cs beam. A dichroic mirror allows for coupling both laser beams into one optical fiber which guides the light into the cryogenic apparatus.

Figure 3 shows the diagnostics used to verify the production of a Cs^* beam. Excitation of the $6S_{1/2} \rightarrow 6P_{3/2}$
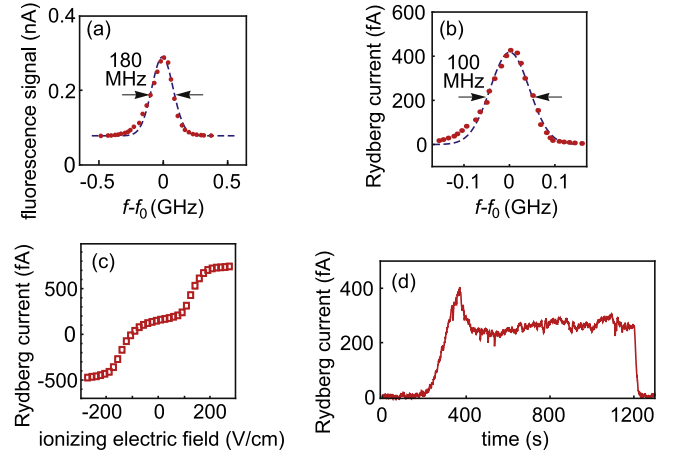

Figure 3. (a) Fluorescence signal as the 852 nm laser is tuned through one of the eight m_I sublevels for the $|6S_{1/2}, m_J = 1/2\rangle \rightarrow |6P_{3/2}, m_J = 3/2\rangle$ transition. (b) Stark-ionization current from Cs^* as the 511 nm laser is scanned across resonance. (c) Stark-ionization current from Cs^* as a function of ionizing electric field. (d) Stark-ionization current as a function of time. After 360 s to allow for the source to heat up, the heating current is reduced by 0.25 A to provide a nearly constant intensity of Cs^*.

transition is verified using fluorescence detection with the InGaAs photodiode shown in figure 1. As Cs has nuclear spin $I = 7/2$, within the presence of a 1-T magnetic field, there are eight nondegenerate m_I sublevels for both the $6S_{1/2}, m_J = 1/2$ and $6P_{3/2}, m_J = 3/2$ states. Figure 3(a) shows the 180 MHz doppler width of the observed fluorescence when tuning through one of the eight ($\Delta m_I = 0$) $|6S_{1/2}, m_J = 1/2\rangle \rightarrow |6P_{3/2}, m_J = 3/2\rangle$ transitions. The 852 nm laser frequency is typically tuned to the $m_I = 7/2$ transition, for Ps^* production experiments.

Excitation to the Rydberg state is verified using a pair of Stark-ionization electrodes (shown in figure 1), which Stark-ionize the Cs^*. Figure 3(b) shows the ionization current as the 511 nm laser is tuned across the 100 MHz wide doppler-broadened resonance. A field of $200\,\text{V cm}^{-1}$ is sufficient to Stark-ionize all of the Cs^*, as shown in figure 3(c), with the resulting ions detected when a positive voltage is used for the ionization, and the electrons collected (leading to a negative current) when a negative voltage is used.

For a typical Ps^* production experiment, the Cs source is first preheated for 360 s, after which the source current is reduced by 0.25 A. This leads to a nearly constant steady-state intensity for the Cs^* beam, as shown in figure 3(d). The typical Stark-ionization current of 250 fA corresponds to 1.6×10^6 Cs^* per second at the location of the ionization electrodes, with only a small fraction of these expected to make it through the small hole into the electrode stack.

4. Production of Rydberg positronium

Ps^* production experiments begin by loading 3×10^7 e^+ obtained [22, 23] from a 50 mCi sealed ^{22}Na source and a buffer-gas accumulator [24] into the cryogenic Penning trap over a period of about 15 min. This is 150 times more than the 2×10^5 e^+ used in the proof-of-principle demonstration [15],
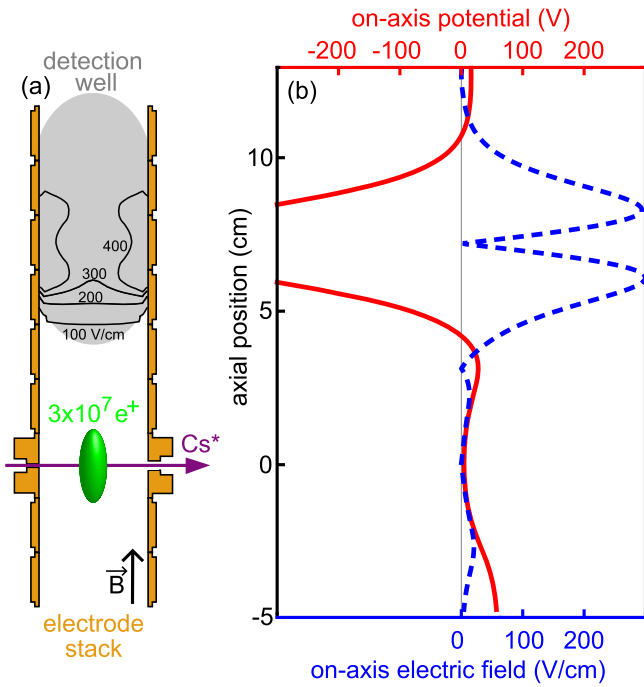
Figure 4. (a) Cross section of the Penning trap electrodes with the location of the positron plasma and the detection well. The gray shaded region depicts the capture volume for this detection well, and the contour lines show the electric fields used to Stark ionize the Ps* atoms. (b) The potential (solid line) and electric fields (dashed line) along the center axis of the Penning trap.
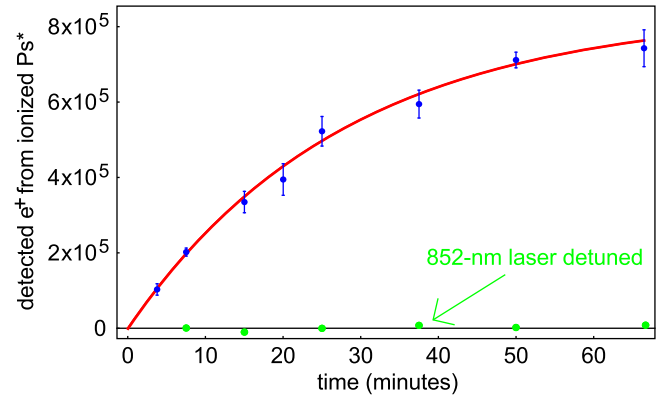

Figure 5. The number of Ps* detected as a function of Cs* beam duration. A fit to a simple exponential function (solid line) indicates a time constant of $1\,680 \pm 100$ s and an initial rate of 500 ± 30 Ps* detected per second. Over 700 000 Ps* are detected for the longest trials. No Ps* production is observed in control trials, for which the 852 nm laser is detuned from resonance.

which used a less efficient method [25] for obtaining e^+. A rotating-wall drive [26] is applied to compress the e^+ to a radius of 4.5 ± 0.5 mm. The e^+ form a nearly ellipsoidal cloud with central density of $\rho_{e^+} = 3 \times 10^7\,cm^{-3}$. This plasma is held in a potential well some distance from the Cs* beam while Cs laser excitations are verified, and then is moved into the potential well shown in figure 4. The potentials used to create this well are chosen to minimize anharmonicity, which could otherwise lead to radial expansion of the e^+ plasma. After the e^+ plasma is in place, the Cs source is again heated, and, when it is producing a nearly constant intensity of Cs, the excitation lasers are allowed to interact with the Cs, and Ps* production begins.

Since the charge exchange is resonant, the Ps* have a binding energy that is approximately equal to that of the Cs*. Thus for $n_{Cs} = 41$ used here, it is expected that n_{Ps} would be approximately $41/\sqrt{2}$. Simulations of the charge exchange [10] indicate a distrubution of n_{Ps} are produced, with values ranging from $n_{Cs}/\sqrt{2}$ down to values that are about 15% lower than this value. Additional collisions of the Cs* or Ps* with e^+ in the plasma might further broaden the distribution of n_{Ps} states.

The deep potential well above the e^+ plasma (the detection well in figure 4) produces electric fields sufficient to ionize Ps* atoms which are traveling through it. The Ps* states are expected to Stark ionize at a distribution of fields (depending on the Stark state) centered at about $(1.5 \times 10^8\,V\,cm^{-1})/n_{Ps}^4$. Most of the Ps* created are expected to ionize between fields of 200 and 400 V cm^{-1}. Electric-field

contours shown in figure 4 indicate the positions at which the Ps* is expected to ionize. The resulting e^+ are captured in the detection well. The e^- from the ionization are repelled from this well and are directed by electrostatic potentials to the bottom of the apparatus. The detection solid angle for the Ps* (the solid angle for which the Ps* gets Stark ionized and the resulting e^+ gets captured in the detection well) depends on the state of Ps*. Averaged over the Ps* states, this solid angle is $2.2 \pm 0.5\%$ of 4π, where the uncertainty results from the uncertain knowledge of the range of Ps* states produced. The potentials for the detection well are designed in such a way that, in the unlikely event that any e^+ not bound in a Ps* atom would enter the detection well, it would make only a single pass through the detection well before exiting the other side.

After the Cs* beam has been introduced into the Penning trap for a specified period of time, the Cs source is turned off and the remaining e^+ plasma is directed to the bottom of the apparatus by inverting the potential well. Following this, the detection well is also inverted (over a 1 s interval) and the number of e^+ in this well is counted. The counting is performed using plastic scintillating fiber detectors, which detect the resulting high-energy e^+-annihilation photons with an efficiency of 0.5%. The fiber counting method is calibrated using comparisons to charge-counting on Faraday cups [23].

Figure 5 shows the number of e^+ collected in the detection well as a function of the time that the Cs* beam is incident on the e^+ plasma. The figure also shows results for experiments with the 852 nm laser detuned from resonance, and, as expected, no e^+ are found in the detection well for these control trials. The Ps* production is initially linear in time (with a rate of 500 ± 30 Ps* per second that are ionized by the detection well) and demonstrates a time constant of 1680 ± 100 s. Both the field-free [10] and the 1-T [14] classical simulations of the charge-exchange process predict that the Ps* will be created with a very nearly isotropic distribution (since both the e^+ in the plasma and the Rydberg e^- orbiting in the Cs* have very nearly isotropic motion). Thus,

the 500 ± 30 Ps* per second that are Stark ionized would indicate that a total of $23\,000 \pm 5000$ Ps* per second are created over the full 4π of solid angle.

Virtually all Cs* are expected to perform a charge exchange with the initial e$^+$ plasma, since

$$\sigma(\text{Ps*})\rho_{e^+} v_{e^+} T_{Cs} > 1. \tag{4}$$

Here $\sigma(\text{Ps}^*)$ is the charge exchange cross section, ρ_{e^+} is the e$^+$ density, v_{e^+} is the e$^+$ speed (which dominates over the much slower speed v_{Cs} of the Cs atoms), and $T_{Cs} = d_{e^+}/v_{Cs}$ is the time that the Cs* spends in the e$^+$ plasma of diameter $d_{e^+} = 9$ mm. Thus, the initial Ps* production rate indicates that $23\,000 \pm 5000$ Cs* per second interact with the e$^+$ plasma. From geometric considerations, along with the fact that approximately 30% of the Cs* radiatively decay to much more tightly bound states before making it to the e$^+$, we estimate that $5 \pm 1\%$ of 1.6×10^6 Cs* per second that make it to the Cs* Stark ionization detector (i.e., $80\,000 \pm 20\,000$ Cs*/s) should make it to the e$^+$ plasma. The two methods of estimating the rate of Cs*-e$^+$ interactions agree to within a factor of about three, and this may be consistent with possible misalignment of the collimators shown in figure 1, which could occur during the cooldown of the apparatus.

Figure 5 indicates that over $700\,000$ Ps* are created within the solid angle addressed by the Stark-ionization detection, which corresponds to 32 ± 7 million Ps* created over the full 4π of solid angle. Thus, almost all of the positrons in the e$^+$ plasma appear to successfully charge exchange into Ps*. It is found that less than 1% of the e$^+$ remain in the initial e$^+$ holding well for the longest trials.

The more than $700\,000$ ionized Ps* represent more than a factor of 500 improvement over the earlier proof-of-principle demonstration of Ps* production [15]. The main factor in this improved number of Ps* is the increased number of e$^+$ available [22, 23] for the current measurement. Larger e$^+$ numbers require deeper potential wells to hold them. Both the deeper potential well and the space charge from the e$^+$ plasma could lead to electric fields that could Stark-ionize the Cs* before it enters the e$^+$ plasma. However, with the three-times-larger-diameter electrodes and larger-sized e$^+$ plasma (figure 1) used in this experiment, these electric fields are small enough to avoid this Stark ionization.

An additional improvement in the current Ps* production is due to greater care in ensuring that high-energy e$^-$ from Stark-ionized Ps* cannot make multiple passes through the e$^+$ well and collisionally heat the e$^+$. These high-energy e$^-$ result from Ps* Stark-ionizing at a large negative potential (as shown in the detection well potentials of figure 4(b)), and thus the resulting e$^-$ pass back through the e$^+$ plasma. For this implementation of Ps* production, the potentials are designed so that the e$^-$ can only make a single pass through the e$^+$ plasma, and therefore the heating is minimized. If the e$^+$ temperature is increased to a point where v_{e^+} exceeds the Cs* Rydberg electron velocity ($v_{e^+} > \alpha c/n \approx 10^4$ m s^{-1}), the cross-section for charge exchange will be significantly reduced [27]. A factor of three of the improved Ps* number can be attributed to the fact that the e$^+$ are not significantly heated by the e$^-$ in this experiment. This factor of three and

the factor of 150 in e$^+$ number are the main factors in the increased number of Ps* produced in this work.

Since the solid angle of Ps* detection for the proof-of-principle demonstration of Ps* production [15] approximately matches the solid angle used here, this work also represents a factor of 500 improvement in the number of Ps* per unit of solid angle near the axis. The number of Ps* per unit solid angle is the figure of merit for producing $\overline{\text{H}}$ from a second charge exchange between Ps* and $\overline{\text{p}}$, and thus a similar improvement factor is expected for $\overline{\text{H}}$ production if a plasma of trapped $\overline{\text{p}}$ replaces the detection well of figure 1.

The factor of 500 improvement in efficiency is especially welcome given the fact that only a very small fraction $N_{\overline{p}}\sigma(\overline{\text{H}})/(4\pi D_{e^+\overline{p}}^2)$ of the Ps* would be expected to form $\overline{\text{H}}$, where $N_{\overline{p}}$ is the number of $\overline{\text{p}}$ available, $\sigma(\overline{\text{H}})$ is the Rydberg charge-exchange cross section for producing $\overline{\text{H}}$, and $D_{e^+\overline{p}}$ is the distance between the e$^+$ and $\overline{\text{p}}$ plasmas. For expected values of $N_{\overline{p}}$ and $D_{e^+\overline{p}}$, this fraction could be as small as 10^{-5}. The kinetic energy of the resulting $\overline{\text{H}}$ would be expected to match that of cold $\overline{\text{p}}$ plasma, which ideally would be cooled to the 1.2 K temperature of the electrodes (or below), with temperatures as cold as 3.5 K [12] and 9 K [13] having already been demonstrated.

5. Conclusions

In this work, a large number of positronium atoms have been created by resonant charge exchange with laser-excited Cs atoms. The binding energy of the Rydberg Ps* atoms is controlled by the laser-excited state of the Cs atom. This production technique may be important for positronium studies of these long-lived states, and will be critical to performing a second charge exchange with $\overline{\text{p}}$ to create large numbers of cold $\overline{\text{H}}$ atoms.

Acknowledgments

References

[1] Gabrielse G, Rolston S L, Haarsma L and Kells W 1988 *Phys. Lett.* A **129** 38
[2] Amoretti M *et al* 2002 *Nature* **419** 456
[3] Gabrielse G *et al* 2002 *Phys. Rev. Lett.* **89** 233401
[4] Enomoto Y *et al* 2010 *Phys. Rev. Lett.* **105** 243401
[5] Kuroda N *et al* 2014 *Nat. Commun.* **5** 3089
[6] Andresen G B *et al* 2010a *Nature* **468** 673
[7] Andresen G B *et al* 2011 *Nat. Phys.* **7** 558
[8] Gabrielse G *et al* 2012 *Phys. Rev. Lett.* **108** 113002
[9] Storry C H *et al* 2004 *Phys. Rev. Lett.* **93** 263401
[10] Hessels E A, Homan D M and Cavagnero M J 1998 *Phys. Rev.* A **57** 1668
[11] Mariazzi S *et al* 2014 *Eur. Phys. J.* D **68** 41

[12] Gabrielse G *et al* 2011 *Phys. Rev. Lett.* **106** 073002
[13] Andresen G B *et al* 2010b *Phys. Rev. Lett.* **105** 013003
[14] Wall M L, Norton C S and Robicheaux F 2005 *Phys. Rev.* A **72** 052702
[15] Speck A, Storry C H, Hessels A E and Gabrielse G 2004 *Phys. Lett.* B **597** 257
[16] Gabrielse G *et al* 2007 *Phys. Rev. Lett.* **98** 113002
[17] Gabrielse G *et al* 2008 *Phys. Rev. Lett.* **100** 113001
[18] Wrubel J *et al* 2011 *Nucl. Instrum. Methods* A **640** 232
[19] Lorenzen C-J and Niemax K 1984 *Z. Phys.* A **315** 127
Sansonetti C J and Lorenzen C-J 1984 *Phys. Rev.* A **30** 1805
[20] Schiff L I and Snyder H 1939 *Phys. Rev.* **55** 59

[21] Müllers A *et al* 2012 *New J. Phys.* **14** 055009
[22] Comeau D *et al* 2012 *New J. Phys.* **14** 045006
[23] Fitzakerley D W *et al* 2016 *J. Phys. B: At. Mol. Opt. Phys.* **49** 064001
[24] Surko C M, Leventhal M and Passner A 1989 *Phys. Rev. Lett.* **62** 901
[25] Estrada J, Roach T, Tan J N, Yesley P and Gabrielse G 2000 *Phys. Rev. Lett.* **84** 859
[26] Anderegg F, Hollmann E M and Driscoll C F 1998 *Phys. Rev. Lett.* **81** 4875
[27] MacAdam K B, Martin N L S, Smith D B, Rolfes R G and Richards D 1986 *Phys. Rev.* A **34** 4661